# Open channel noise

## V. Fluctuating barriers to ion entry in gramicidin A channels

Stefan H. Heinemann*‡ and Frederick J. Sigworth‡

*Max-Planck-Institut für biophysikalische Chemie, Abteilung Membranbiophysik, D-3400 Göttingen, Federal Republic of Germany; and ‡Department of Cellular and Molecular Physiology, Yale University School of Medicine, New Haven, Connecticut 06510

ABSTRACT We have measured the fluctuations in the current through gramicidin A (GA) channels in symmetrical solutions of monovalent cations of various concentrations, and compared the spectral density values with those computed using E. Frehland's theory for noise in discrete transport systems (Frehland, E. 1978. *Biophys. Chem.* 8:255–265). The noise for the transport of $NH_4^+$ and $Na^+$ ions in glycerol-monooleate/squalene membranes could be accounted for entirely by "shot noise" in the process of transport through a single-filing pore with two ion binding sites. However, in confirmation of results in a previous paper (Sigworth, F. J., D. W. Urry, and K. U. Prasad. 1987. *Biophys. J.* 52:1055–1064) currents of $Cs^+$ showed a substantial excess noise at low ion concentrations, as did currents of $K^+$ and $Rb^+$. The excess noise was increased in thicker membranes. The observations are accounted for by a theory that postulates fluctuations of the entry rates of ions into the channel on a time scale of $\sim 1$ $\mu$s. These fluctuations occur preferentially when the channel is empty; the presence of bound ions stabilizes the "high conductance" conformation of the channel. The fluctuations are sensed to different degrees by the various ion species, and their kinetics depend on membrane thickness.

## INTRODUCTION

The transport of ions through a membrane channel has been traditionally described as a process of discrete jumps of ions over energy barriers in a static, rigid pore. However, molecular dynamics simulations of permeation in the gramicidin A (GA) channel (e.g., Fischer and Brickmann, 1983; Mackay et al., 1984: Kim et al., 1985; Etchebest and Pullman, 1986*a* and *b*; Skerra and Brickmann, 1987) suggest that motions of coordinating groups in the GA channel, on time scales of picoseconds to nanoseconds, are essential to the ion transport process. It has also been suggested that structural fluctuations on longer time scales, resulting in "fluctuating barriers" to ion transport, may also be important in determining the transport properties of a channel (Läuger, 1983; Eisenman, 1987).

The present series of papers has been concerned with experiments to characterize the fluctuations in ion current through "open" membrane channels. Some current fluctuations are expected to arise from the discrete nature of the current flow (individual ions move in discrete steps across the membrane), yielding "shot noise" analogous to that seen in electronic devices. Additional noise would be expected if the ion-transport process is modulated, e.g., by fluctuating barriers (Läuger et al., 1980). Measurements of currents in acetylcholine receptor channels (Auerbach and Sachs, 1983; Sigworth, 1985, 1986) as well as measurements made on other channel types (Eisenberg et al., 1988, 1989) reveal fluctuations in excess of shot noise which are likely to arise from internal motions of the channel protein. Subsequent experiments with channels formed by GA and several analogues also showed spectral density values several times that expected from shot noise (Sigworth et al., 1987). These measurements were made on $Cs^+$ currents with the GA channels in diphytanoyl phosphatidylcholine/decane membranes, and showed a constant spectral density within the range of measurement (up to 20 kHz) suggesting that the time scale of underlying structural fluctuations would be shorter than $\sim 5$ $\mu$s.

The ion transport process in GA channels has been studied intensively (see, for example, Finkelstein and Andersen, 1981; Hladky and Haydon, 1984) and the channel structure, a head-to-head dimer of beta helices, has been well established (Urry, 1971; Urry et al., 1983; Arseniev et al., 1985). Thus we felt that if we could determine the time scale of the excess current fluctuations, and which steps in the ion transport process were important in causing them, we could begin to assign the structural basis of the fluctuations. We have not been able to determine the time scale directly, because our measurements of GA channel noise have been limited to a bandwidth of 20 kHz. However, we have started to compare our measured spectral densities with the predictions from specific kinetic schemes for ion transport, using the theory of Frehland (1978, 1980). In the calculations we take the "low-frequency" limit corresponding to


0006-3495/90/03/499/16 $2.00

our accessible frequency range, but nevertheless can obtain estimates at relevant time scales by comparing theory with experimental data obtained at various ion concentrations.

In a first application of this approach, calculations were performed using two standard models for GA ion transport: the three-barrier, two-site transport [3B2S] model of Finkelstein and Andersen (1981); and the three-barrier, four-binding site [3B4S] model of Eisenman and Sandblom (1983). These calculations failed to predict the large current fluctuations that were observed (Sigworth and Shenkel, 1988). We then extended the 3B2S model to explicitly include blocking steps in the transport scheme and were able to estimate blocking dwell times of ~100 ns for formamide molecules in the GA channel (Heinemann and Sigworth, 1988) and dwell times of ~12 ns of $Na^+$ in the channel based on induced noise in $H^+$ currents (Heinemann and Sigworth, 1989). In the course of these two studies we noticed that $Na^+$ and $K^+$ currents with GA channels in glycerol-monooleate (GMO)/squalene membranes actually had noise spectral densities below the classical shot noise values; this is a behavior predicted by the 3B2S and 3B4S models.

Thus it appeared to us that ion transport fluctuations might depend on ion species and membrane composition, as well as ionic strength. In the present work we have therefore studied the concentration dependence of mean currents and noise in GA channels using GMO/squalene membranes and solutions of $NH_4Cl$, NaCl, KCl, RbCl, and CsCl. Further, presuming that the dependence of fluctuations on membrane composition may occur through the membrane thickness, we performed experiments with lipids of various chain lengths. We describe the results in terms of an extended version of the 3B2S model which simultaneously describes the single-channel current and spectral density observed under these various conditions. The model implies that the excess current fluctuations arise from structural fluctuations at the channel entrances.

## METHODS

### High-resolution recordings from microbilayers

Artificial bilayers were formed on pipette tips (3–5 μm diameter) and the currents through GA channels were recorded as described by Sigworth et al. (1987). In most experiments the lipid was 40 mg/ml GMO in squalene. To determine the influence of membrane thickness on the open-channel current spectra, monoglycerides with longer and shorter chain lengths were used. Lipids were obtained from Nu Chek Prep, Inc., Elysian, MN. Squalene and other solvents were obtained from Sigma Chemical Co., St. Louis, MO. Chloride solutions of $NH_4^+$, $Na^+$, $K^+$, $Rb^+$, and $Cs^+$ in Millipore-filtered water were used. Optical grade CsCl (Sigma Chemical Co.) was used; it was found to yield more stable membranes.

### Open channel noise analysis

The open-channel current noise was analyzed as previously described (Sigworth, 1985). Closing events of durations as short as ~10 μs were masked out before calculating the Fourier transform in blocks of 1,024 data points sampled at 44.1 kHz. The resulting power spectra, corrected for the transfer function of the recording system, were averaged in sets according to the number of channels open at the corresponding time.

## THEORY

### Current noise in a discrete transport system

The ion conduction through channels can be modeled as a transport system having discrete states connected by transition rates. A state is defined by the ion occupancy (i.e., which of the discrete binding sites in the channel are occupied by ions) and sometimes also by the conformational state of the channel protein. As an example, consider the transport of a single ion in a channel with two binding sites, which consists of the following three steps. First there is a transition from the empty channel state to a state in which one site is occupied by an ion (association of an ion with a binding site); then a transition to another state with the ion at the site at the opposite end of the channel (translocation of the ion); finally, a transition back to the empty state (ion dissociates).

Treating this model as a Markov process, time development of the probability $\langle n_i \rangle$ of being in each state $i$ is given by a master equation,

$$\frac{d\langle n_i \rangle}{dt} = \sum_{j=1}^{n} m_{ij} \langle n_j \rangle, \tag{1}$$

where $m_{ij}$ is the transition rate from state $j$ to state $i$. Solutions to this equation can be used to obtain steady-state measures such as channel occupancy or mean current under given conditions.

The spectral density $S_i$ of the fluctuations in the channel current at thermodynamic equilibrium (i.e., with zero net current) can be obtained by calculating the electrical admittance of the system, $Y$, and subsequent application of Nyquist's formula (Nyquist, 1928; Läuger, 1978):

$$S_i(f) = 4kT\mathrm{Re}\{Y\}. \tag{2}$$

Single-channel experiments are usually carried out far from the thermodynamic equilibrium, because a voltage gradient is applied to generate a measurable ion current. For this case we use the more general treatment of discrete transport systems by Frehland (1978, 1980). A summary of Frehland's theory and an outline of our numerical implementation of it has been given by Heinemann and Sigworth (1988); we show here a derivation of

the final expression for the spectral density of the current fluctuation, which is subject to our measurements. Let $\alpha_i = n_i - \langle n_i \rangle$ be the fluctuation away from the mean value of the occupancy of a given state. The $\alpha_i$ satisfy

$$\frac{d\langle \alpha_i \rangle}{dt} = \sum_{j=1}^{n} m_{ij} \langle \alpha_j \rangle. \quad (3)$$

Current fluctuations are related to fluctuations in state occupancies through the transition rates $m_{ij}$ and the corresponding amount of charge, $\gamma_{ij}$, transferred across the membrane with each transition. The autocovariance $c(t)$ of the current fluctuations is then computed according to the temporal correlations of impulses of current arising from individual transitions,

$$c(t) = \sum_{i,j,k,l=1}^{n} \gamma_{ij}\gamma_{kl} m_{ij} \langle n_j \rangle [\delta_{ij,kl}\delta(t) + m_{kl}\omega_{li}(t)], \quad (4)$$

where the contribution of all pairs of transitions $l \rightarrow k$ and $j \rightarrow i$ is summed; $\delta_{ij,kl}$ is the general Kronecker symbol, $\delta(t)$ is Dirac's function, and $\omega_{li}$ is the solution of the master Eq. 3 for occupancy fluctuations of state $l$ given the initial condition of state $i$. The spectral density of the current is then obtained by Fourier transformation of Eq. 4 according to the Wiener-Khinchine theorem.

$$S_i(f) = \sum_{i,j,k,l=1}^{n} \gamma_{ij}\gamma_{kl} m_{ij} \langle n_j \rangle \left[ 2\delta_{ij,kl} + 4m_{kl} \int_0^\infty \omega_{li}(t) \cos(2\pi f t)\, dt \right]. \quad (5)$$

In the limit of zero frequency, which is the limit of interest to us, the integral can be evaluated readily by making use of the inverse of the transition matrix $M$.

## Examples of current noise

Before we consider the behavior of the GA channel we first consider the noise in the simple ion-transport processes shown in Fig. 1.

### Shot noise

The classical theory of shot noise (Schottky, 1918) assumes that charge transport is unidirectional, occurs in an instantaneous process, and that the charge movements are uncorrelated in time (that is, they occur as a Poisson process; Fig. 1 *A*). The spectral density of the fluctuations is then given by Schottky's formula,

$$S_{Shot} = 2iq. \quad (6)$$

The spectral density is proportional to the single-channel current $i$ and the charge $q$ of the transported ion, and does not depend on frequency. Because of its simple relationship to the channel current, we normalize our experimental spectral density values to $S_{Shot}$.

### Blocking noise

Interruptions in the simple shot process by a blocking mechanism, modeled here as an energy barrier that gates the transport by switching between two levels (Fig. 1 *B*), yields an excess noise with a Lorentzian characteristic. Given the mean duration, $\tau$, and a frequency, $\lambda$, of the

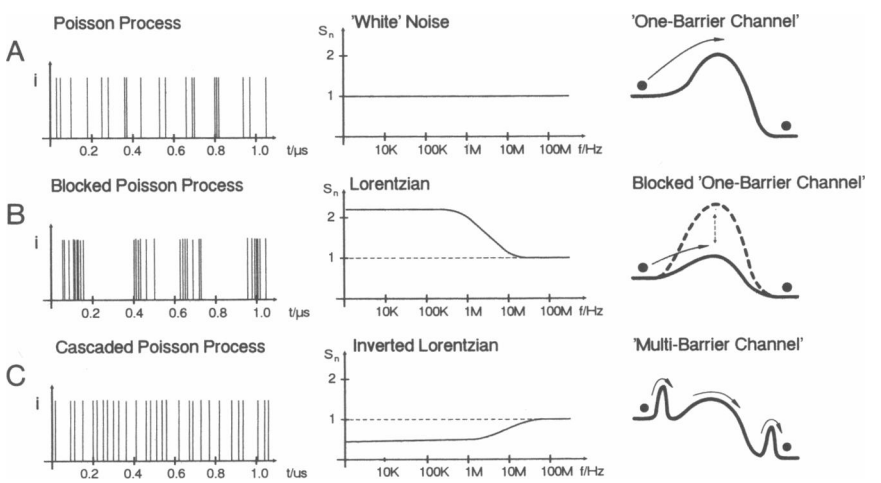


FIGURE 1 Illustration of microscopic currents and noise spectra from three simple mechanisms of ion transport. (*A*) A transport mechanism having one rate-limiting barrier. The impulses of current corresponding to ion transport events occur as a Poisson process, and the corresponding power spectrum is independent of the frequency. (*B*) A similar process, but interrupted by blocking events which generate excess noise having a Lorentzian power spectrum. (*C*) A single-ion channel with multiple barriers. The individual ion-transport events are more evenly spaced in time than in *A*, producing a decreased spectral density at low frequencies.

blocking events, the power spectrum can be approximated by (Sigworth et al., 1987)

$$S_i(f) = 2iq + 4\lambda\tau^2 i^2 \frac{1}{1 + (2\pi f\tau)^2}. \quad (7)$$

### Multistep transport

One expects that if ions pass through a channel in multiple steps, each moving the ion through only a fraction of the width of the membrane, the result will be less transport noise than in the simple shot process (Frehland and Stephan, 1979). Less obvious, perhaps, is the reduction in noise in a multistep process even when the electrical charge movement is confined to a single step (Fig. 1 *C*). In this case we assume ion–ion interactions (e.g., a single-occupancy channel) so that one ion must wait for some time after the preceding ion has contributed its pulse of current; this temporal anticorrelation results in a lower spectral density at low frequencies.

Each of the spectra in Fig. 1 is seen to approach a constant spectral density equal to the classical shot noise at high frequencies. This behavior holds only if individual shot events are δ-functions. Because the ions require a finite time to jump from one site to the next, the actual spectra are expected to roll off at a frequency of some gigahertz, corresponding to the actual transit time.

## Noise expected from models of gramicidin

The transport of ions through the GA channel is known to occur in a multistep process, in which ions cannot pass each other inside the pore (single filing). Kinetic schemes corresponding to two popular models for transport in GA channels are shown in Fig. 2. Fig. 2 *A* shows the four-state model for a channel having a binding site at each end (Finkelstein and Andersen, 1981). Although this model successfully describes the main features of ion transport, there is evidence that the ions sense two more sites close to the channel mouths (Eisenman and Sandblom, 1983). A simplification of such a four-site model is shown in Fig. 2 *B*. To account for the electrical repulsion of ions in close proximity, the maximum occupancy of the channel is restricted to two ions, and it is assumed that neighboring binding sites cannot be occupied simultaneously (Sandblom et al., 1983). With these restrictions the number of possible states of the channel is reduced from 16 to eight.

Fig. 3 presents the predicted ion concentration dependence and voltage dependence of the low-frequency noise spectral density, the single-channel current, and the degree of ion occupancy of the channel for these two

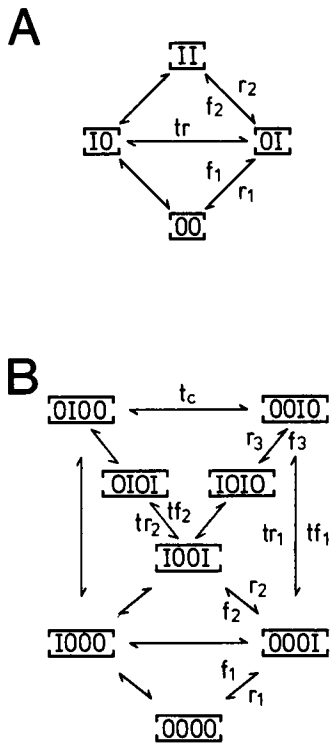


FIGURE 2 Possible models for ion permeation through the GA channel. The boxes denote the channel pore, with '0' representing an empty ion binding site, and 'I' an ion occupying a site. (*A*) The two-site model after Finkelstein and Andersen (1981). (*B*) A simplified version of the four-site model of Eisenman and Sandblom (1983), which includes two additional sites close to the channel mouths. The model is simplified by the assumptions that only two ions can occupy the channel at a time, and two neighboring binding sites may not be simultaneously occupied (Sandblom et al., 1983).

kinetic models. For simplicity in this calculation all ion association rates were set equal, as were the various dissociation rates and the translocation rates (see the legend for values). The energy profiles for the passage of one ion, which indicate the position of the binding sites in the electric field, are shown as insets in the figure. For both the two-site model (Fig. 3 *A*) and the four-site model (Fig. 3 *B*) it is seen that the single-channel current saturates at high ion concentrations. The noise ratio (the ratio of the zero-frequency spectral density to $S_{Shot}$) approaches unity at low ion concentrations and goes through a minimum at concentrations where the channel is approximately half-occupied by ions.

The concentration dependence of the noise ratio can be understood as follows. At low concentrations the single rate-limiting step is the association of an ion with the channel; once associated the various transport steps occur in rapid succession, such that at low time resolution (i.e., low frequencies) they together appear to result in a single

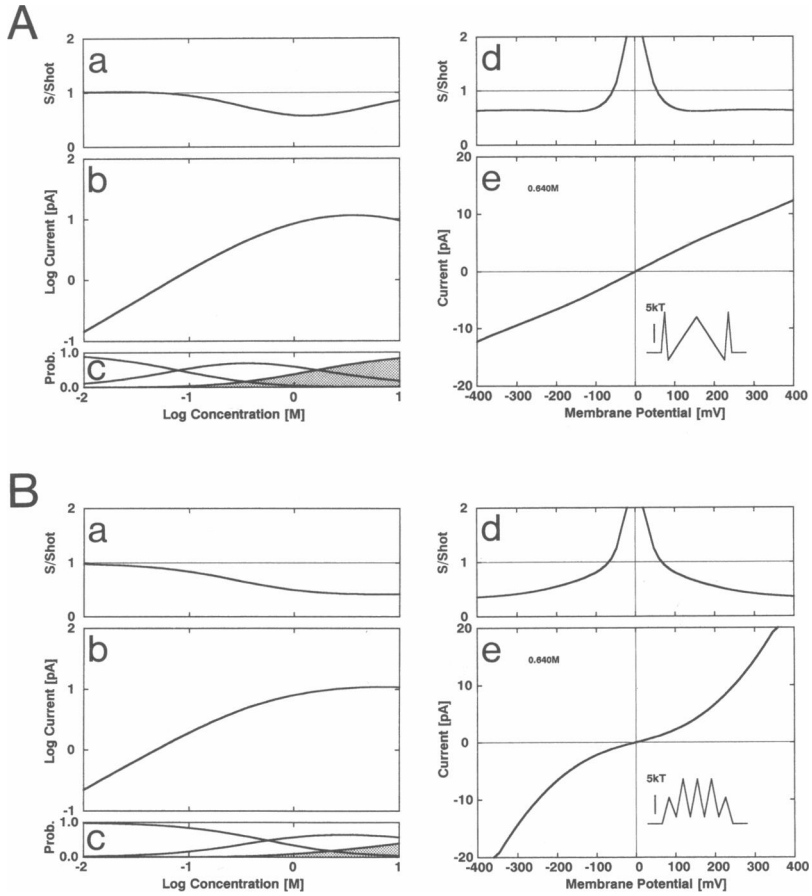


FIGURE 3 Concentration dependence and voltage dependence of noise for (*A*) the two-site model, and (*B*) the four-site model of Fig. 2. The permeation characteristics were calculated for symmetrical ionic conditions. In panel *a* of each part of the figure the zero-frequency limit of the noise ratio $S/S_{Shot}$ is plotted as a function of ion concentration at 200 mV membrane potential. The ratio is unity at low ion concentrations but falls substantially below unity at intermediate and high concentrations due to the presence of multiple rate-limiting steps, as in Fig. 1 *C*. The corresponding mean current (*b*) and channel occupancy probabilities (*c*) are also shown as functions of concentration. The probability of finding the channel occupied by two ions is indicated by the shaded area. Voltage dependences of the noise ratio (*d*) and mean current (*e*) are shown for an ion concentration of 640 mM. The noise ratio diverges as the voltage approaches zero, because the equilibrium thermal noise (2) does not vanish whereas $S_{shot}$ does when $i = 0$ (Eq. 6). In *A* the two-site model was used with $f_1 = f_2 = 6.0 \times 10^7\ s^{-1}\ mol^{-1}$, $r_1 = r_2 = 7.0 \times 10^6\ s^{-1}$, and $t = 2.6 \times 10^7\ s^{-1}$. In *B* the four-site model had all association rates $f_i = 3.4 \times 10^9\ s^{-1}\ mol^{-1}$, the dissociation rates $r_i = 2.4 \times 10^{10}\ s^{-1}$, and the translocation rates $t_i = 1.2 \times 10^8\ s^{-1}$. The apparent energy profiles for one ion are shown in the insets which also illustrate the position of the binding sites in the electric field.

pulse of current with area $q$. This is equivalent to the classical shot noise process, and so yields a noise ratio of unity. At higher concentrations the association rate and various other transport rates become comparable in magnitude. Because of the single-file nature of the transport, we have the case as in Fig. 1 C where one ion must wait a significant interval while another ion is being transported. This results in a reduction of the low-frequency spectral density below $S_{Shot}$.

The right panels of Fig. 3 show the dependence of the single-channel current and $S/S_{Shot}$ on the membrane potential at a fixed ion concentration (640 mM). The noise ratio diverges as the voltage approaches zero potential, as would be expected because we normalize the spectral density to the Schottky noise (Eq. 6) which, because it assumes a unidirectional ion flux, does not contain the equilibrium thermal noise (Eq. 2).

Thus the main feature predicted by both of the popular schemes for GA ion permeation is a reduction in the noise ratio when the channel occupancy becomes appreciable. Given the correct model, the particular concentration dependence of the noise ratio would allow estimates to be made for the relative values of rates that, being in the range of $10^7\ s^{-1}$, are too rapid to be observed directly. Neither of these models predicts a noise ratio greater than unity at high potentials (i.e., >100 mV) and therefore will

need to be modified to describe those cases where excess noise is observed experimentally.

## RESULTS

### Ion dependence of channel transport noise

Currents through GA channels show brief interruptions (gaps) with mean duration ~ 10 μs and a frequency of occurrence that depends on the solvent used for preparing the lipid bilayers (Sigworth and Shenkel, 1988). These gaps, if not properly masked from the recording before calculating the power spectrum, would give rise to a considerable excess noise as described by Eq. 7. Assuming that this effect depends on membrane thickness, we used GMO/squalene membranes, which are thin and almost solvent free (White, 1978; Waldbillig and Szabo, 1979). With these membranes the frequency of brief interruptions is reduced to ~ 1–2 $s^{-1}$ which, after our standard masking procedure, is expected to make a negligible contamination of the spectra.

Fig. 4 *A* shows data traces of $K^+$ (left panel) and $Cs^+$ (right panel) currents in the vicinity of channel closing events, each plotted on two different time scales. In the trace of $Cs^+$ current typical brief closings and a closing through an intermediate step are seen. Similar events are also seen when the current is carried by other cations. The two panels in Fig. 4 *B* show superimposed power spectra of the baseline and the open-channel currents, whose differences (Fig. 4 *C*) are taken to be the channel noise

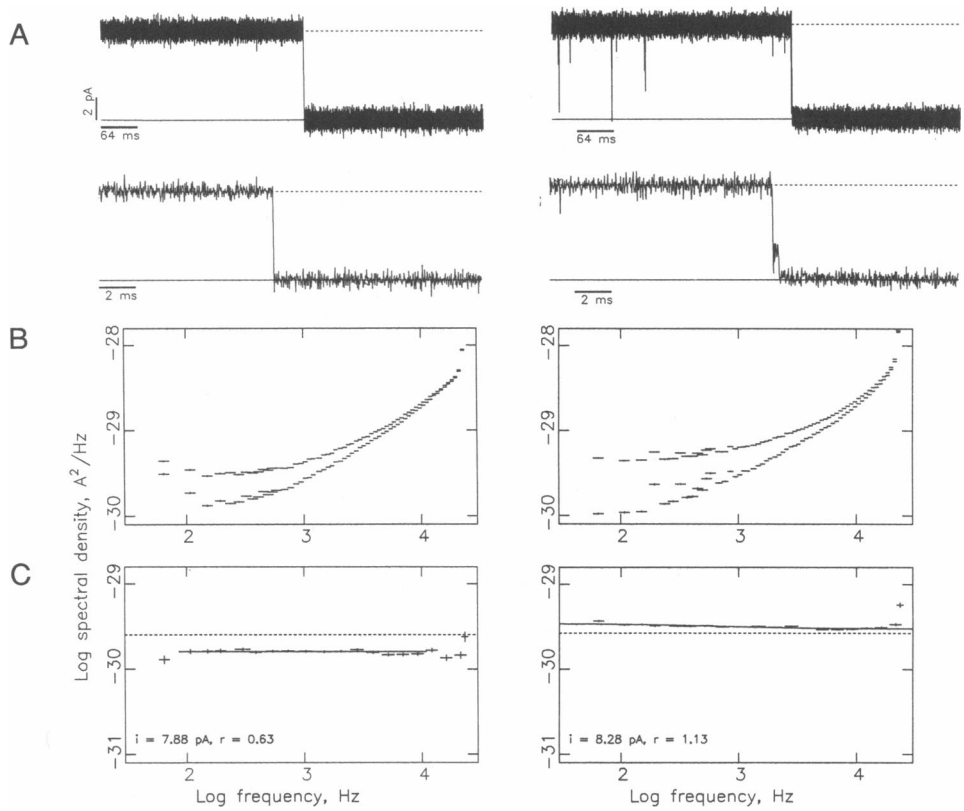


FIGURE 4 Single-channel current events and open-channel spectra in 640 mM KCl (*left*) and 320 mM CsCl (*right*) with GMO/squalene membranes at 200 mV. (*A*) Single-channel closing events at two different time scales. On the CsCl trace several brief gaps are visible, as is a "step-closing" event shown on the high-resolution trace. Before computing spectra, gaps are eliminated by the masking procedure as mentioned in the Methods. At the full 10 kHz bandwidth used for the display here, the large background noise obscures the increase in noise when a channel is open. (*B*) Average power spectra computed from 100–1,000 segments of 1,024 samples of open-channel current (*upper points*) and baseline current. (*C*) Difference spectra, obtained by subtracting the data in part *B*. The spectral density for $K^+$ currents was estimated as the average of the spectral values (shown as a line) over the range of 0.1 to 10 kHz, yielding $1.6 \times 10^{-30}$ $A^2$/Hz. In some cases, however, the spectra showed a slight frequency dependence, as in the $Cs^+$ data here. The transport noise spectral density $S$ was computed from a fit to the data with the function $S + S_1/(1 + f/f_c)$. From a fit over the frequency range of 0.04 to 15 kHz the parameters were $S = 3.00 \times 10^{-30}$ $A^2$/Hz, $S_1 = 4.39 \times 10^{-31}$ $A^2$/Hz, and $f_c = 590$ Hz. The contamination of the transport noise estimate by the decaying component at 10 kHz is therefore < 1%.

spectra. The difference spectrum in 640 mM KCl (left panel) is flat, and the spectral density is lower than the Schottky noise level (dashed line) by a ratio of 0.63. The spectrum for 320 mM CsCl is not completely flat; there is a slight decay with increasing frequency. This phenomenon was not seen in every experiment, and no dependence on either ion species, ionic strength, or membrane potential was found. To estimate the asymptotic shot noise level the spectra showing such a decay were fitted by the sum of a constant and a small component proportional to $1/f$ (for details refer to caption of Fig. 4). Because the values of the constant component were repeatable, we used them as measures of the ion transport noise for further calculations. In the spectrum shown the noise ratio is 1.13. Note that, despite the large difference in transport noise, the single-channel currents in these two experiments are very similar.

Corresponding experiments were performed for $NH_4^+$, $Na^+$, $K^+$, $Rb^+$, and $Cs^+$ at various ion concentrations and membrane potentials. Fig. 5 presents the results for each ion along with sets of curves computed, as in Fig. 3 from models of the permeation process. The concentration dependences of noise ratio and current are shown from measurements at 200 mV, whereas the voltage dependences were from measurements at 640 mM salt concentration (1.0 M for $Na^+$).

In the cases of $NH_4^+$ and $Na^+$ the measured noise ratio is lower than 1.0 in the concentration and voltage range explored. A fit to these data of the four-state model of Fig. 2 *A* (dotted curves) resulted in a quite satisfactory match, suggesting that the observed noise in currents of these ions arise only from the transport process, with no excess resulting from protein fluctuations. However, in currents of $K^+$, $Rb^+$, and $Cs^+$ the noise ratio increased considerably above unity at low ion concentrations; as we have seen, neither of the two models of Fig. 2 predicts ratios > 1.

An explanation for an increase in noise at low ion concentrations would be a conformational fluctuation that occurs preferentially when the channel is empty. This is illustrated in Fig. 6 *A*, where the concentration dependence of the spectral density is compared for three different kinds of stepwise reductions in permeation rates, occurring at mean frequencies of $\sim 1.0 \times 10^4\ s^{-1}$ and lasting $\sim 1\ \mu s$. The solid curve shows the prediction of a scheme in which the ion entry rate can switch from its normal value to a lower one for brief periods while the channel is empty. The excess spectral density (shaded region) is largest at low concentrations where the ion-association step is rate-limiting in the permeation process. On the other hand, the noise from rapid channel "gating" (dotted curve), here assumed to have kinetics that are independent of the ion-occupancy state, is larger at higher concentrations because it is proportional to $i^2$ (Eq. 7). Excess noise from a fluctuating central barrier (dashed curve) shows an even steeper increase at high concentrations because only in that region do the translocation rates across the barrier become rate limiting for ion transport.

The model for a fluctuating ion-entry rate which yielded the solid curve in Fig. 6 *A* is illustrated in Fig. 6 *B*. The four-state model was extended with an additional state [00]* which can be accessed only from the "normal" empty-channel state [00]. We take this "blocked" state to represent a conformation of the empty channel that can receive ions only at the reduced association rate $f_1^*$. For a first attempt we assumed that the equilibrium between the two empty states is solely described by the rate $\lambda$ of entry into [00]* and the dwell time $\tau$ in that state; that is, $f_1^*$ was set to zero. Fits to this model resulted in much better descriptions of the concentration dependence of the spectral density. However, a problem with the fits was that $\lambda$ and $\tau$ had to vary depending on the ion species, which is unreasonable because the channel is not occupied by ions while the fluctuation between [00] and [00]* takes place. We then allowed $f_1^*$ to take nonzero values depending on the ion species, and sought values for $\lambda$ and $\tau$ that were independent of species.

To fit the data with the five-state model, we first set $f_1^*$ to zero to estimate the required magnitude of $\lambda$ and $\tau$ (see below). Then for the fits, shown as solid curves in each part of Fig. 5, we kept these parameters constant at $\lambda = 3.5 \times 10^4\ s^{-1}$ and $\tau = 3.0\ \mu s$. Even with these constraints we obtained better fits than with the model lacking the $f_1^*$ transition. The sets of parameters obtained in the fits for each ion species are listed in Table 1.

The dotted curves in Fig. 5 were calculated in each case from the corresponding four-state model (by setting $\lambda$ to zero). It should be noted that although the addition of the blocked state of the channel causes a substantial increase in the noise, it makes little change in the channel current. Dotted curves as plotted in the panels of Fig. 5 are showing the current values from the four-state model, but they are indistinguishable from the solid curves.

## Channel noise is influenced by lipid environment

Because a blocked state is likely to result from a structural change of the channel, we wondered if the transitions into this state might depend on physical parameters of the membrane, such as membrane thickness. The membrane thickness and the solvent content of the membrane have a strong influence on the kinetics of dimerization (e.g., Elliott et al., 1983) as well as on kinetic features at faster time scales (Sigworth and Shenkel, 1988). We therefore performed experiments using monoglycerides

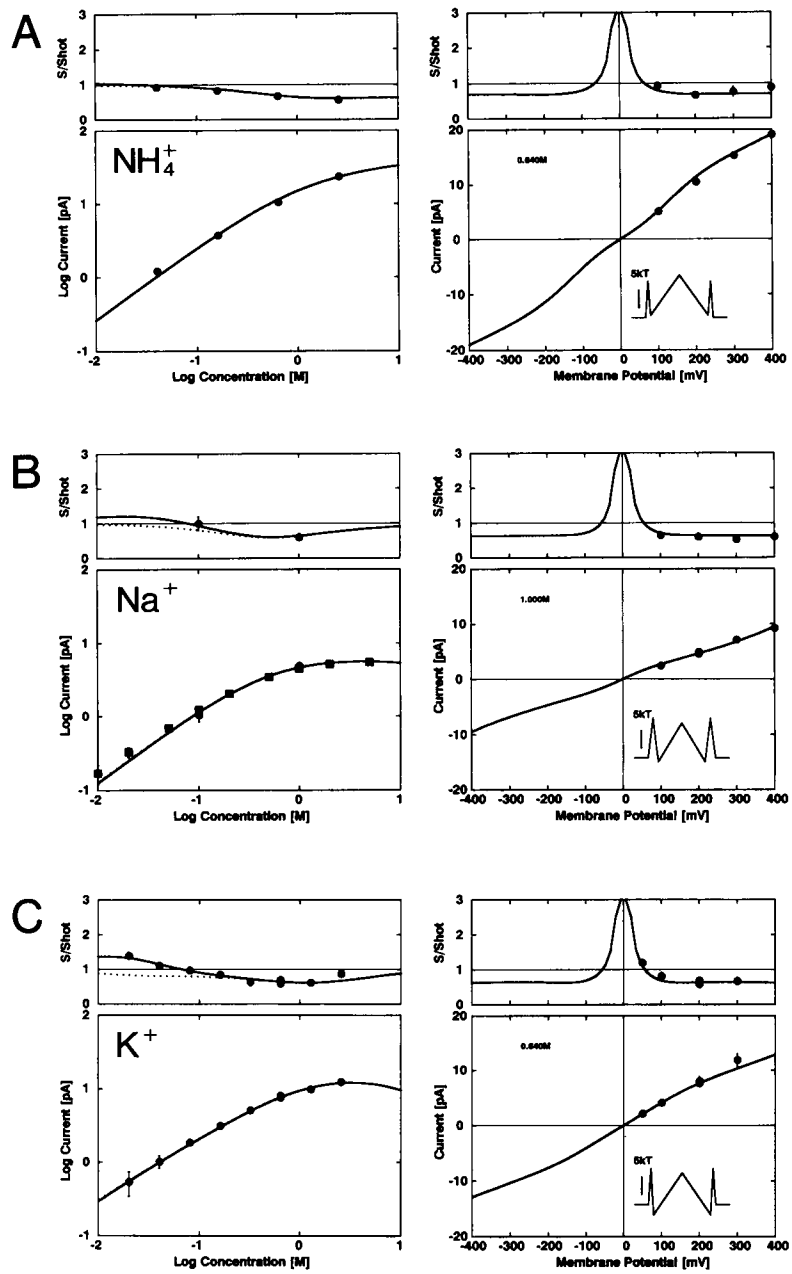


FIGURE 5 Noise ratio and channel currents as functions of concentration and voltage for permeation by $NH_4^+$, $Na^+$, $K^+$, $Rb^+$, and $Cs^+$ in GMO-squalene membranes. Data are displayed in the format of Fig. 3. Points are experimental values obtained from one to three experiments, with error bars indicating ± SEM; some of the sodium current values (*squares*) were taken from Neher et al. (1978). Right panels show the noise ratios and single-channel currents as a function of voltage at 640 mM salt concentration (1.0 M for $Na^+$), and the insets show effective energy-barrier representations. The solid curves are fits of the five-state permeation model (Fig. 6) to the data with the transition rates to the blocked state fixed at $\tau = 3.0\ \mu s$ and $\lambda = 3.5 \times 10^4\ s^{-1}$. The dotted curves were calculated for the four-state model (Fig. 2 *A*) with the same parameters ($\lambda$ was simply set to zero in the five-state model). Dotted curves are included, but superimpose almost exactly over the solid curves, in the plots of channel current as a function of concentration and voltage. It can be seen the four-state model describes the noise ratio well for $NH_4^+$ and $Na^+$, but predicts too little noise for $K^+$, $Rb^+$, and $Cs^+$. In the least-squares fitting the $S/S_{Shot}$ values were weighted equally, whereas the squared error in each current value $i$ was weighted by $\sim 1/|i|$. The fitted parameters are listed in Table 1, except for the case of $Rb^+$, where the few data points did not sufficiently constrain the parameters. The curves shown for $Rb^+$ were obtained by a free fit of the transport parameters: $f_1 = 1.8 \times 10^8\ s^{-1}\ mol^{-1}$, $r_1 = 9.0 \times 10^6\ s^{-1}$, $t_r = 8.4 \times 10^7\ s^{-1}$, $f_2 = 1.4 \times 10^8\ s^{-1}\ mol^{-1}$, $r_2 = 2.5 \times 10^8\ s^{-1}$, $f_1^* = 3.7 \times 10^5\ s^{-1}\ mol^{-1}$.

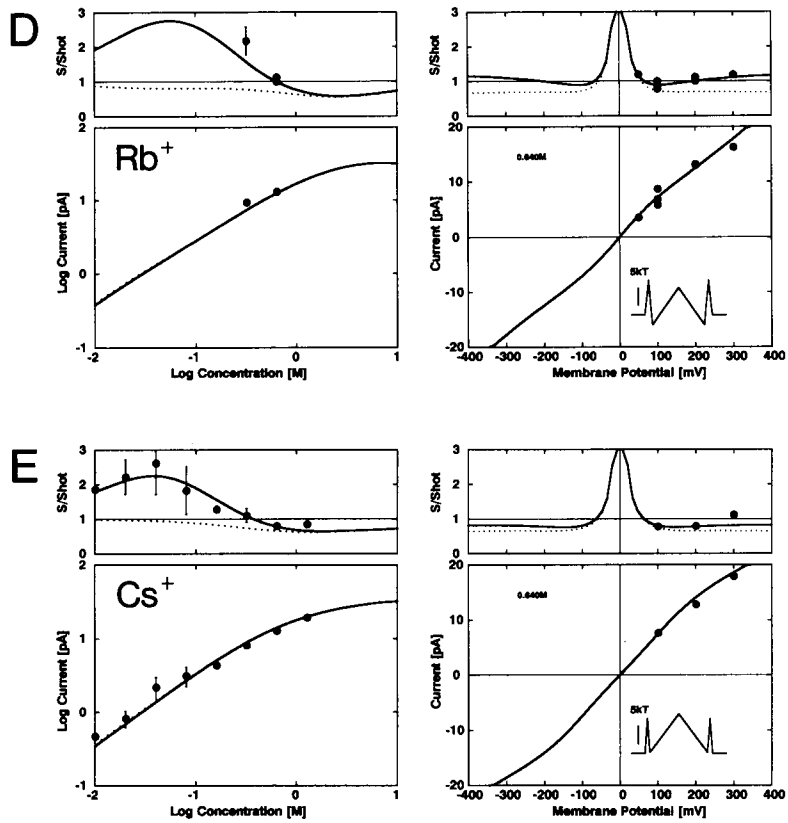


FIGURE 5 (continued)

with various chain lengths, and experiments with GMO membranes containing hexadecane and decane instead of squalene. In Fig. 7 the results in KCl solutions are summarized. Data were obtained with membranes from GMPalmitolein (C 1:16), GMOlein (C 1:18), GMEisocein (C 1:20), and GMErucin (C 1:22) in squalene; also an experiment with GMO (C 1:18) in decane is shown. The recording with GMErucin was obtained at 27°C because of its higher melting point; the other experiments were carried out at room temperature.

The curves in Fig. 7 were drawn using the same parameters as for the KCl data in Fig. 6, but with changes in the transition rates involving the blocking step. The entry rate $f_1^*$ was set to zero, leaving only $\lambda$ and $\tau$ to vary to fit the data. As in the preceding figure, dotted curves show the corresponding results for the four-state model. The noise ratio values in the thinnest membranes (C 1:16) were so low that the four-state model was sufficient to describe the data. With increasing chain length, however, $\lambda$ and $\tau$ had to be increased to describe the increasing noise. Only a few data points were obtained for the long-chain lipids, but the noise ratio is seen to clearly increase with chain length, from 0.53 in GMPalmitolein to 1.06 in GMErucin in 640 mM KCl at 200 mV.

In fitting the data in Fig. 7 we found that the parameters $\lambda$ and $\tau$ were not independently constrained by the available data. However, the quantity $\lambda\tau^2$ was well defined; it is a rough measure for the low-frequency excess noise generated by a blocking mechanism (Eq. 7). The fitted and measured values for $S/S_{\text{Shot}}$ are plotted in Fig. 8 as a function of membrane thickness (open symbols), with the thickness values obtained from the literature (Kolb and Bamberg, 1977; Rudnev et al., 1981; Hladky and Gruen, 1982; Elliott et al., 1983). The squares in Fig. 8 show the parameters determined from GMO/decane membranes. The noise ratio $S/S_{\text{Shot}}$ appears to saturate, as do the fitted values of $\lambda$ and $\tau$ (at roughly $4.0 \times 10^4$ s$^{-1}$ and 1.5–2.0 $\mu$s, respectively) for thick membranes. The saturation is likely a result of the masking procedure which we apply to eliminate time-resolved, brief channel closures. An estimate of this effect is shown in the Appendix.

A similar series of experiments was performed with CsCl solutions, as summarized in Fig. 9 (note that the data points in Fig. 9 were not obtained under identical experimental conditions). For reasons of limited membrane stability the experiments were more difficult to perform in CsCl than in KCl, and these data have a wide

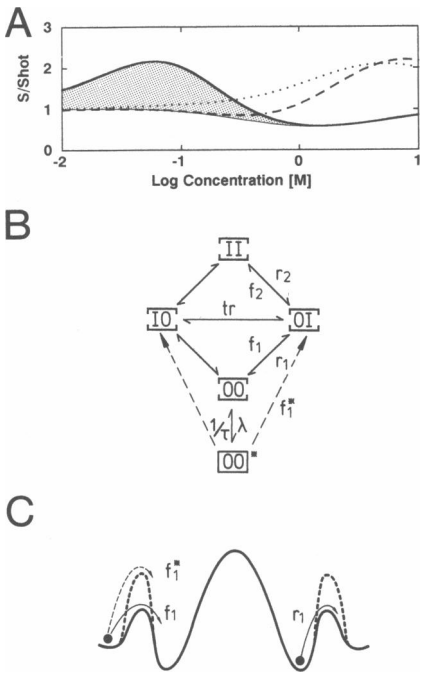


FIGURE 6 Noise from fluctuating barrier models. (*A*) Predictions of $S/S_{Shot}$ as function of ion concentration, using the same parameters and four-state model as in Fig. 3 *A a*, but assuming that stepwise fluctuations occur in certain rates of the ion transport scheme. Fluctuating entry barriers (*solid curve*) cause an excess noise at low ion concentrations (*shaded area*) as compared with the four-state model. A fluctuating central barrier (*dashed curve*), in which the translocation rates $t_r$ vanish for a mean time $\tau = 1$ μs at a mean rate of $1.7 \times 10^4$ s$^{-1}$, yields excess current noise only at high ion concentrations. A simple gating process (*dotted curve*), in which the channel current is interrupted regardless of the channel occupation state for 1 μs at a mean rate of $1.0 \times 10^4$ s$^{-1}$, also results in excess noise at higher concentrations. (*B*) The four-state model (Finkelstein and Andersen, 1981) has been extended to include the blocked state [00]*. The channel can relax into this state only from the unoccupied state [00]. The states [00] and [00]* are distinguished by their corresponding entry rates for ions. When $f_1^*$ is comparable to $f_1$, then the effective state model becomes similar to the four-state model (Fig. 2 *A*). Channel blockage due to a much smaller $f_1^*$ results in the observed excess noise at low ion concentrations. The solid curve in *A* was computed using this scheme with $\lambda = 4.5 \times 10^4$ s$^{-1}$, $\tau = 3$ μs and $f_1^* = 1.0 \times 10^6$ s$^{-1}$. (*C*) The state diagram of *B* can be translated into an energy profile (shown here for a single ion) having fluctuating entry barrier heights.

scatter. Nevertheless, a similar tendency to increased channel block is seen with increasing membrane thickness.

## DISCUSSION

### GA channels can act like rigid pores

Under certain conditions the current noise in GA channels can be accounted for entirely by the "shot noise"

**TABLE 1 Rate constants for $NH_4$, Na, K, and Cs for the five-state model**

| Rate | $NH_4^+$ | $Na^+$ | $K^+$ | $Cs^+$ |
|---|---|---|---|---|
| $s^{-1}$ | | | | |
| $f_1 \times$ mol$^{-1}$ | $1.4 \times 10^8$ | $4.6 \times 10^7$ | $1.6 \times 10^8$ | $1.9 \times 10^8$ |
| $r_1$ | $2.8 \times 10^8$ | $1.5 \times 10^7$ | $8.2 \times 10^6$ | $2.7 \times 10^8$ |
| $t_r$ | $4.5 \times 10^7$ | $6.5 \times 10^7$ | $2.9 \times 10^7$ | $6.7 \times 10^7$ |
| $f_2 \times$ mol$^{-1}$ | $1.7 \times 10^7$ | $3.9 \times 10^7$ | $1.3 \times 10^8$ | $2.1 \times 10^7$ |
| $r_2$ | $3.9 \times 10^8$ | $2.4 \times 10^7$ | $1.1 \times 10^8$ | $2.3 \times 10^8$ |
| $f_1^* \times$ mol$^{-1}$ | $4.0 \times 10^7$ | $5.2 \times 10^6$ | $4.9 \times 10^6$ | $4.1 \times 10^6$ |
| $\delta$ | 0.079 | 0.153 | 0.079 | 0.074 |

Rate constants for the two-site, five-state model (Fig. 6) obtained in the simultaneous fits, shown in Fig. 5, to measurements of channel current and spectral density at various membrane potentials and concentrations of the permeating ions. The relative position $\delta$ of the binding site in the electric field is also given for each case. The data were obtained in GMO/squalene membranes at room temperature. In the fits the equilibrium between the states [00] and [00]* was kept constant, with the parameters $\lambda = 3.5 \times 10^4$ s$^{-1}$, $\tau = 3.0$ μs.

expected from the discrete transport of ions through a rigid pore. In this respect the currents carried by $NH_4^+$ and $Na^+$ in GMO/squalene membranes, and by $K^+$ in the thinner GMP membranes are well described by the two-site, four-state model of Finkelstein and Andersen (1981), or alternatively by the more elaborate model of Eisenman and Sandblom (1983). These models predict spectral densities lower than classical Schottky noise (Eq. 6) at intermediate ion concentrations because of the multiple steps in the ion transport process, and such a reduction in the noise ratio is in fact observed.

The lack of excess current fluctuations suggests a remarkable lack of structural fluctuations, because minor changes in amino acid side chains have been shown to have dramatic effects on ion permeation (Andersen et al., 1987; Becker et al., 1989). Besides the lack of rapid fluctuations the channel current shows only occasional sublevels and brief gaps of ~ 1 ms and ~ 10 μs, respectively (Ring, 1986; Sigworth and Shenkel, 1988), while the lifetime of the GA dimer in a thin membrane is ~ 10 s. Thus it appears that the GA channel is essentially a rigid pore on time scales from seconds down to the dwell times for ion transport, ~ 10–100 ns, and the conduction process must also be little affected by fluctuations in the lipid environment on this time scale (Hladky and Gruen, 1982; Crawford and Earnshaw, 1987). Our measurements can say little about structural fluctuations on time scales <10 ns, which however are likely to be substantial. The lowest normal mode frequencies of the GA dimer are ~ $10^{11}$ Hz (Roux and Karplus, 1988), and librations of the peptide carbonyl groups on the time scale of ~1 ps are expected to be important in the motion of an ion through the channel (Fischer and Brickmann, 1983; Urry et al., 1984*b*).

The low current noise in the GA channel is a property

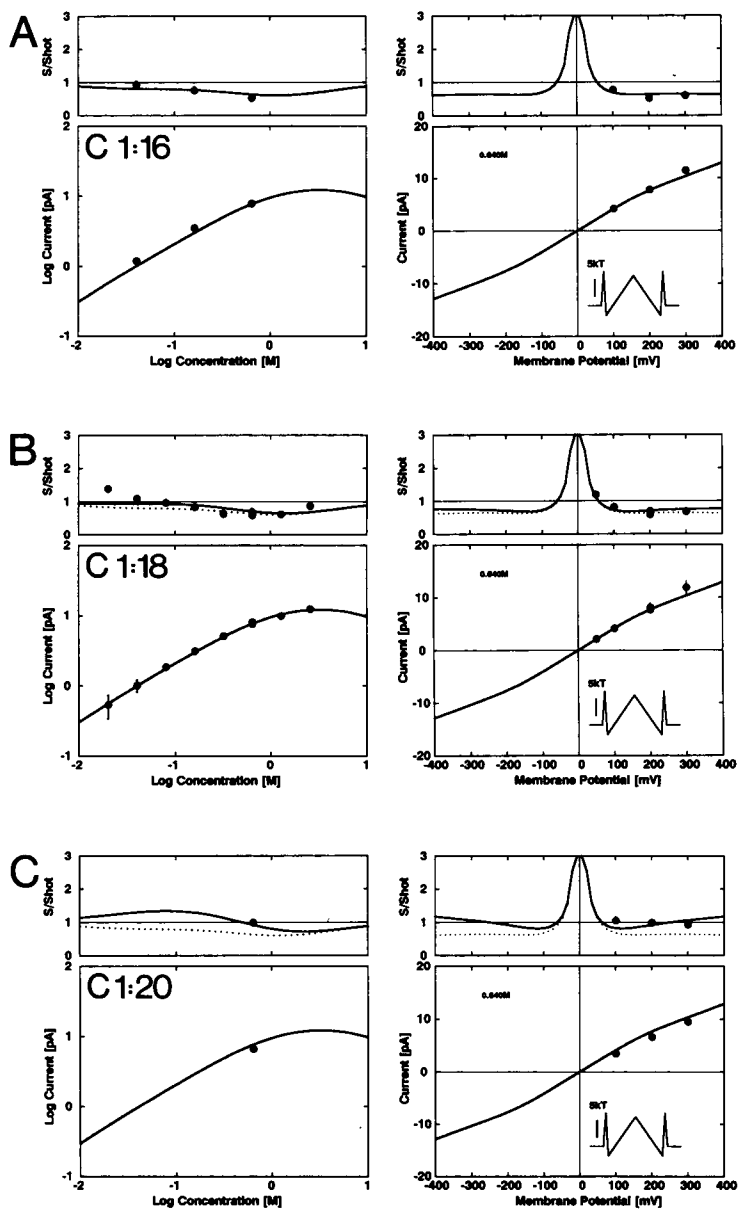


FIGURE 7 Noise ratio and channel currents in KCl with membranes of various thicknesses. Data are displayed in the format of Fig. 3 for membranes formed with GMPalmitolein (C 1:16), GMO (C 1:18), GMEisocein (C 1:20), and GMErucin (C 1:22) in squalene (40 mg/ml). Data from one experiment with GMO in decane (C18/decane) are also shown. The experiments with GMErucin were performed at 27°C. Theoretical curves for the five-state (*solid*) and four-state (*dotted*) models are shown as in Fig. 5; they were calculated from the parameters for $K^+$ currents in GMO/squalene membranes (Table 1 and Fig. 5). The dotted curves are identical in each case. The solid curves were fitted by varying only the blocking parameters $\lambda$ and $\tau$, whereas $f_1^*$ was set to zero. It is seen that the noise ratio becomes larger as the lipid chain length is increased. A large increase in noise is also seen with decane as the membrane solvent, which yields thicker membranes.

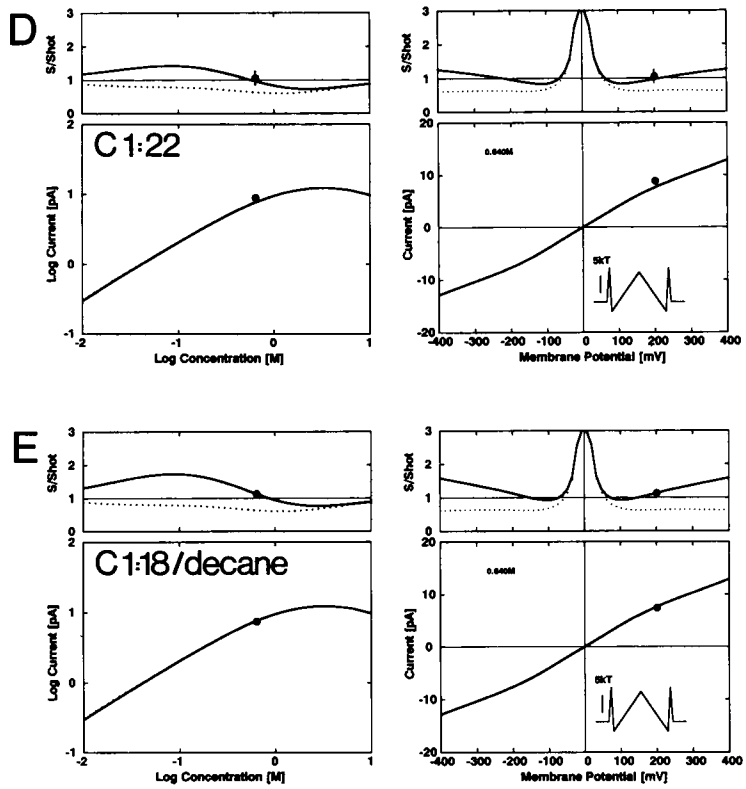


FIGURE 7 (continued)

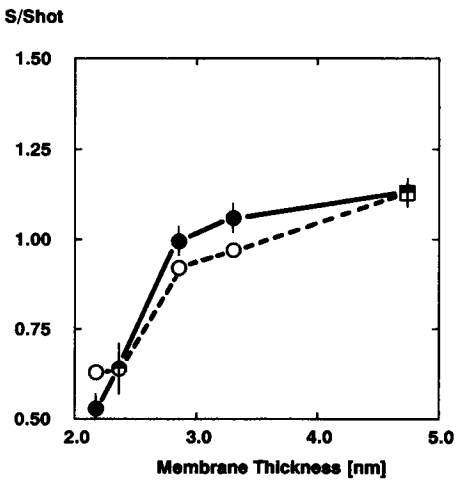


FIGURE 8 Measured (*solid symbols*) and fitted (*open symbols*) $S/S_{Shot}$ in 640 mM KCl and at 200 mV membrane potential as function of the estimated membrane thickness at room temperature. The squares denote experiments in GMO/decane. The estimates for $\tau$ and $\lambda$ range from $< 5.0 \times 10^{-8}$ s and $<600\ s^{-1}$ for the thinnest membranes to $1.9 \times 10^{-6}$ s and $4.5 \times 10^{4}\ s^{-1}$ for GMO/decane membranes. Estimates for membrane thickness were obtained from the literature (Kolb and Bamberg, 1977; Rudnev et al., 1981; Hladky and Gruen, 1982; Elliott et al., 1983).

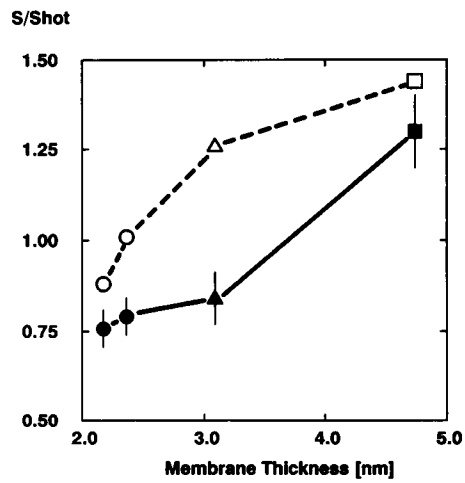


FIGURE 9 Measured (*solid symbols*) and fitted (*open symbols*) $S/S_{Shot}$ as function of the estimated membrane thickness at 200 mV and room temperature. The circles represent experiments in 640 mM CsCl with squalene as solvent; the triangles denote experiments in GMO/hexadecane and 500 mM CsCl, the squares represent experiments of L-Ala$^7$-GA in diphytanoyl phosphatidylcholine/decane membranes and 1.0 M CsCl (Sigworth et al., 1987). The estimates for $\tau$ and $\lambda$ range from $1.7 \times 10^{-6}$ s and $2.7 \times 10^{4}\ s^{-1}$ for GMP membranes to $3.3 \times 10^{-6}$ s and $3.9 \times 10^{4}\ s^{-1}$ for the data with L-Ala$^7$-GA.

that is not shared by other channels that have been investigated in this way. High-frequency (~10 kHz) spectral densities several times the shot noise level are observed in the acetylcholine receptor channel (Sigworth, 1985), a cation channel in frog lens epithelium (Eisenberg et al., 1988) and a potassium channel of lobster sarcoplasmic reticulum (Eisenberg et al., 1989). Currents in these channels also show low-frequency excess noise that is suggestive of millisecond time scale fluctuations.

## Ion-dependent excess noise

Under some conditions the currents in the GA channel can show noise spectral densities several times that expected for simple shot noise, as has been pointed out previously (Sigworth et al., 1987; Sigworth and Shenkel, 1988). The excess noise appears at relatively low ion concentrations, and is larger for $Rb^+$ and $Cs^+$ than for the smaller alkali metal cations and $NH_4^+$. We have interpreted our data in terms of a five-state model which successfully explains the concentration dependence of the noise. This model extends the standard two-site, four-state scheme to include, besides the unoccupied state [00] of the "conducting" channel, a second unoccupied state [00]* that is "blocked"; that is, it allows ion entry only at a reduced rate. The physical picture is that of a channel whose structure is stabilized in the conducting conformation when it is occupied by one or more ions, but when it is empty it can relax into the blocked conformation. The stabilization of the channel conformation by ions has already been suggested by Ring and Sandblom (1988) in studies of the lifetime of the GA dimer, and could be involved in the possible ion-dependent dissociation of GA aggregates observed by Urry et al. (1984*a*) in bilayers containing a high concentration of GA.

In fitting the model to the data obtained with GMO/squalene membranes and various ions, we described the conformational transitions of the channel with the rate $\lambda = 3.5 \times 10^4\ s^{-1}$ of entering the blocked state, and the dwell time $\tau = 3.0\ \mu s$ in the blocked state at limiting low ion concentration. The remaining parameters that were fitted are given in Table 1 for each ion species. The rates $f_1$ for ion association with the empty but unblocked channel ranged from $5 \times 10^7$ to $2 \times 10^8\ M^{-1}s^{-1}$. The corresponding rates $f_1^*$ for association with the blocked channel were all near $5 \times 10^6$, with the exception of $NH_4^+$, whose $f_1^*$ value was an order of magnitude higher.

In the context of the model the particularly large noise observed with $Cs^+$ can be understood from the large value of $f_1$, allowing relatively large currents to flow at low $Cs^+$ concentrations, and the large rates of transport $t_r$ and dissociation $r_1$ which allow transported ions to exit quickly and leave the channel empty most of the time. Thus the large $Cs^+$ currents are often interrupted by transitions to the blocked state, which require an empty channel. On the other hand the lower noise in $Na^+$ currents is explained by lower association and dissociation rates, resulting in smaller fluxes that are interrupted less often. $NH_4^+$ currents are remarkable because they are as large as currents with $Cs^+$ but have very low noise. In terms of the model, the explanation for the low noise is that $f_1^*$ is much higher, comparable to $f_1$. Thus while the other ion species see a substantial fluctuation in the barrier to entry into the channel, the entry rate of $NH_4^+$ is little influenced by the state of the channel.

## Thick membranes destabilize the GA channel

A large increase in excess noise was observed when the membrane thickness was increased either by using longer-chain lipids or changing the solvent. The increase can be explained by a shift in the equilibrium from the state [00] to the blocked state [00]*, presumably as mechanical stress due to the thicker membranes destabilizes the channel structure. This picture has an analogy in the slow kinetics of dimerization, because the channel lifetime depends strongly on the bilayer thickness (Kolb and Bamberg, 1977; Rudnev et al., 1981; Elliott et al., 1983). The explanation for the lifetime variation is that the monomers can be separated by forces arising from the mismatch between bilayer thickness and channel length. Hydromechanical models for the deformation free energy of lipid bilayers containing surface tension, bilayer compressibility, and splay distortion have shown quantitative agreement with this idea (Huang, 1986; Helfrich and Jakobsson, 1988). It is therefore tempting to assume a similar mechanism for the description of the rapid transitions that give rise to the excess noise that we observe.

Besides this rather static mechanism in which a thick membrane pulls the GA molecules or parts of it apart to cause fluctuations, another possibility is that fluctuations in the lipid matrix are coupled directly to the ion permeation process. Hladky and Gruen (1982) predicted an rms thickness fluctuation that increases strongly if squalene is replaced by decane as solvent. The relaxation times of fluctuations in lipid bilayers are in an appropriate range to give rise to the current fluctuations. The formation of *gauche* conformations in the lipid acyl chains has a relaxation time of ~5 $\mu s$, for example (Crawford and Earnshaw, 1987).

## Time scale of fluctuations

The magnitude of the excess spectral density readily leads to an estimate of the product $\lambda \tau^2$, but an estimate of $\lambda$ or $\tau$

alone, to give an idea of the time scale of the fluctuations, is more difficult to obtain. In our fitting procedure we have obtained estimates of these parameters from the concentration dependence of the noise spectral density. Intuitively one expects that the excess fluctuations due to channel block will vanish when the block time becomes shorter than the time between ion transport events. Since the rate of transport varies with the ion concentration, the detailed dependence of spectral density on concentration should therefore reflect the time scale of block. More direct measurements of the block time are likely to be possible in the future through the analysis of higher moments of the fluctuation amplitude distribution, or by measuring power spectra at higher frequencies.

The value of $\sim 3$ $\mu$s that we obtain for $\tau$ means that the blocking events are tantalizingly close to being directly observable in recordings of channel currents. As predicted by the five-state model, however, the blocking events are shortened by ion entry (via the rate $f_1^*$) at the higher concentrations where the channel currents are large and short events can best be detected. For example, the large excess noise in 100 mM CsCl apparently arises from $\sim 1$ $\mu$s blocking events, much shorter than our $\sim 10$ $\mu$s limit for detectable current interruptions. On the other hand, the brief gaps whose frequency of occurrence increases dramatically in thick membranes (Sigworth and Shenkel, 1988; also see Appendix) are likely to be dwells in the blocked state, made visible by a lengthening of $\tau$.

## What forms the fluctuating barrier?

The evidence for a fluctuating barrier to ion entry is the observation of excess noise at low ion concentrations, as seen in the present work and in the preceding paper in this series (Sigworth et al., 1987). It should be noted that a fluctuating barrier is not required to describe the mean channel current and its dependence on concentration or voltage; indeed, the currents predicted by the five-state model are indistinguishable from the values predicted when the model is reduced to the standard four-state form (Figs. 5 and 7). The five-state model we have used is very successful in accounting for the concentration dependence of the excess noise. This model is perhaps the simplest but certainly not the only model that can describe the data. A more elaborate model certainly would need to consider four binding sites for ions (Sandblom et al., 1983) and fluctuations of the energy profile. As a minimum requirement, however, some sort of fluctuation or blocking process is clearly necessary to account for the excess noise that we have characterized here.

A difficulty with the five-state model is its implication that the structural change that yields the blocked state is not confined to the ends of the channel. The blocked state must arise from a global change of the channel structure, since it simultaneously prevents ion entry at both ends of the channel, and is allowed only when ions are absent from both ends of the channel. Consider an alternative model in which each end of the channel behaves independently, making a transition with rate $\lambda'$ to raise its barrier whenever its binding site is empty (Fig. 10). This scheme has potentially many more free parameters, but for simplicity we assume that the ion entry rate is the only rate influenced by the structural transition of an end of the channel. Even with these constraints the predictions of this model are essentially identical to those of the five-state model. The probability of the new, ion-occupied blocked states (OI] and [IO) is very low because the rates of leaving these states are much higher than $\lambda'$: specifically, the rapid translocation rate $t_r$ allows an ion, if present anywhere in the channel, to effectively keep both ends of the channel out of the blocked state. Thus this model is functionally equivalent to the five-state model but supports the appealing physical picture of local, rather than global, structural fluctuations.

What part of the channel structure likely causes the fluctuating barrier? Similar levels of excess noise are observed in gramicidin analogues that are modified at positions 5–8, i.e., near the middle of the polypeptide chains (Sigworth et al., 1987); recordings from covalently linked gramicidin dimers (Heinemann, S. H., C. J. Stankovic, and S. L. Schreiber, unpublished results) also show excess noise. These results suggest that the fluctuations are not confined to central parts of the GA dimer and do not arise as part of the process of dissociation of the dimeric channel. The most likely site for the underlying structural fluctuations is the region of the COOH-

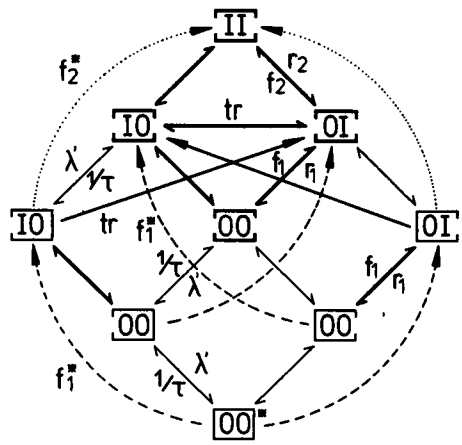


FIGURE 10 Extension of the 3B2S model to allow independent blockage of each channel end. Ion association with blocked ends is represented by dashed arcs. Setting $\lambda' = \lambda/2$ and $f_2^* = 0$ yields predictions very similar to those of the five-state model of Fig. 6.

terminus of each GA monomer, which forms the mouth of the channel. In this respect it is interesting to consider the case of $NH_4^+$, whose entry is little affected by the fluctuating barrier. $NH_4^+$ differs from the alkali ions in its ability to form hydrogen bonds, and so may be better coordinated in a transition state for entry into the channel.

From computer simulations it appears that the dynamics of the ethanolamine end group has a strong influence on the association of ions with the binding site (Etchebest and Pullman, 1986*b*). One can imagine that the movements of this group, together with forces at the lipid-water interface, could result in the reversible breakage of the first one or two intrahelical hydrogen bonds. This may cause a poor coordination of entering ions (which in the case of $NH_4^+$ is overcome by its ability to form H-bonds with the channel structure) or even a partial channel block by the ethanolamine moiety itself. Investigation of changes in the COOH-terminal group of GA, which by this hypothesis would have a strong effect on the open-channel noise, might therefore shed some light on the interactions between the channel protein and the lipid-water interface.

Another possibility is that the observed fluctuations arise from the reorientation of the side chains of the tryptophan residues which are located near the ion binding sites. Such a mechanism was suggested as the basis for low-conductance states of the channel having lifetimes on the order of seconds (Urry et al., 1984*c*), but is also likely to occur on a much shorter time scale. One expects that channels in which phenylalanine is substituted for tryptophan (Becker et al., 1989) would show substantially different noise characteristics if this hypothesis were true.

## APPENDIX

The derived parameters of the blocking equilibrium appear to saturate for thick membranes, as shown in Fig. 8. This is most likely an effect of the masking procedure which we applied to the recorded data to remove brief channel closures before computing the spectrum (Sigworth, 1985). In this appendix we estimate the magnitude of the effect of masking on the spectral density due to brief closing events.

Let the measured noise $S(0)$ be entirely generated by a blocking mechanism, parameterized by $\lambda$ and $\tau$. Then we would measure

$$S(0) = 4\lambda\tau^2 i^2, \tag{8}$$

without masking, where $i$ is the single-channel amplitude. If all closing events longer than $t_m$ are eliminated, there remains a reduced spectral density.

$$S_m(0) = 2\lambda_m \langle t_m^2 \rangle i^2 \tag{9}$$

with

$$\lambda_m = \lambda \int_0^{t_m} \frac{1}{\tau} \exp^{-t/\tau} dt \tag{10}$$

**TABLE 2 Effect of masking on measured excess noise**

| | $\tau$ | | |
|---|---|---|---|
| $t_m$ | 1.5 μs | 2.5 μs | 3.5 μs |
| 8 μs | 1.116 | 1.681 | 2.782 |
| 10 μs | 1.041 | 1.337 | 1.950 |
| 12 μs | 1.014 | 1.105 | 1.552 |

Ratio $S(0)/S_m(0)$ for various masking cutoff times $t_m$ and mean block dwell times $\tau$.

$$\langle t_m^2 \rangle = \int_0^{t_m} t^2 \frac{1}{\tau} \exp^{-t/\tau} dt. \tag{11}$$

In Table 2 the ratio $S(0)/S_m(0)$ is shown for various masking criteria and block time constants. It is seen for $\tau = 3.5$ μs the measured parameters as shown in Fig. 8 are subject to an underestimation by a factor of ~2.

We thank Drs. E. Neher and M. Pusch for carefully reading the manuscript, and D. Urry and K. Prasad for providing the gramicidin samples.

This work was supported by National Institutes of Health grant NS-21051. S. H. Heinemann was partly supported by the German Academic Exchange Service and a Max-Planck stipend.

*Received for publication 28 August 1989 and in final form 20 November 1989.*

## REFERENCES

Andersen, O. S., R. E. Koeppe II, J. T. Durkin, and J.-L. Mazet. 1987. Structure-function studies on linear gramicidins. Site-specific modifications in a membrane channel. *In* Ion Transport through Membranes. K. Yagi and B. Pullman, editors. Academic Press, Inc., Tokyo. 295–314.

Arseniev, A. S., I. L. Barsukov, V. F. Bystrov, A. L. Lomize, and Yu. A. Ovchinnikov. 1985. $^1$H-NMR study of gramicidin A transmembrane ion channel. Head-to-head right-handed, single-stranded helices. *FEBS (Fed. Eur. Biochem. Soc.) Lett.* 186:168–174.

Auerbach, A., and F. Sachs. 1983. Flickering of a nicotinic ion channel to a subconductance state. *Biophys. J.* 42:1–10.

Becker, M. D., D. B. Sawyer, A. K. Maddock, R. E. Koeppe II, and O. S. Andersen. 1989. Single tryptophan-to-phenylalanine substitutions in gramicidin channels. *Biophys. J.* 55:503a. (Abstr.)

Crawford, G. E., and J. C. Earnshaw. 1987. Viscoelastic relaxation of bilayer lipid membranes. Frequency-dependent tension and membrane viscosity. *Biophys. J.* 52:87–94.

Eisenberg, R. S., A. H. Hainsworth, and R. A. Levis. 1988. Open-channel noise in a cation channel of frog lens epithelium. *J. Physiol. (Lond.)*396:84P.

Eisenberg, R. S., A. H. Hainsworth, and R. A. Levis. 1989. The effect of temperature on open-channel noise in the potassium channel of lobster sarcoplasmatic reticulum. *J. Physiol. (Lond.)* 410:18P.

Eisenman, G. 1987. Electrical signs of rapid fluctuations in the energy profile of an open channel. *In* Ion Transport through Membranes. K. Yagi and B. Pullman, editors. Academic Press, Inc., Tokyo. 101–129.

Eisenman, G., and J. P. Sandblom. 1983. Energy barriers in ionic channels: data for gramicidin A interpreted using a single-file (3B4S") model having 3 barriers separating 4 sites. *In* Physical Chemistry of Transmembrane Ion Motions. G. Spach, editor. Elsevier Science Publishers, Amsterdam. 329–348.

Elliott, J. R., D. Needham, J. P. Dilger, and D. A. Haydon. 1983. The effects of bilayer thickness and tension on gramicidin single-channel lifetime. *Biochim. Biophys. Acta.* 735:95–103.

Etchebest, C., and A. Pullman. 1986*a*. The gramicidin A channel: energetics and structural characteristics of the progression of a sodium ion in the presence of water. *J. Biomol. Struct & Dyn.* 3:805–825.

Etchebest, C., and A. Pullman. 1986*b*. The gramicidin A channel. The energy profile for $Na^+$ in the presence of water with inclusion of the flexibility of the ethanolamine tail. *Fed. Eur. Biochem. Soc. Lett.* 204:261–265.

Finkelstein, A., and O. S. Andersen. 1981. The gramicidin A channel: a review of its permeability characteristics with special reference to the single-file aspect of transport. *J. Membr. Biol.* 59:155–171.

Fischer, W., and J. Brickmann. 1983. Ion-specific diffusion rates through transmembrane protein channels. A molecular dynamics study. *Biophys. Chem.* 18:323–337.

Frehland, E. 1978. Current noise around steady states in discrete transport systems. *Biophys. Chem.* 8:255–265.

Frehland, E. 1980. Current fluctuations in discrete transport systems far from equilibrium. Breakdown of the fluctuation dissipation theorem. *Biophys. Chem.* 12:63–71.

Frehland, E., and W. Stephan. 1979. Theory of single-file noise. *Biochim. Biophys. Acta.* 553:326–341.

Heinemann, S. H., and F. J. Sigworth. 1988. Open channel noise. IV. Estimation of rapid kinetics of formamide block in gramicidin A channels. *Biophys. J.* 54:757–764.

Heinemann, S. H., and F. J. Sigworth. 1989. Estimation of $Na^+$ dwell time in the gramicidin A channel. Na ions as blockers of $H^+$ currents. *Biochim. Biophys. Acta.* 987:8–14.

Helfrich, P., and E. Jakobsson. 1988. Calculation of deformation energies and conformations in lipid membranes containing gramicidin channels. *Biophys. J.* 53:327a. (Abstr.)

Hladky, S. B., and D. W. R. Gruen. 1982. Thickness fluctuations in black lipid membranes. *Biophys. J.* 38:251–258.

Hladky, S. B., and D. A. Haydon. 1984. Ion movements in gramicidin channels. *Curr. Top. Membr. Transp.* 21:327–372.

Huang, W. H. 1986. Deformation free energy of bilayer membrane and its effect on gramicidin channel lifetime. *Biophys. J.* 50:1061–1070.

Kim, K. S., D. P. Vercauteren, M. Welti, S. Chin, and E. Clementi. 1985. Interaction of $K^+$ ion with the solvated gramicidin A transmembrane channel. *Biophys. J.* 47:327–335.

Kolb, H.-A., and E. Bamberg. 1977. Influence of membrane thickness and ion concentration on the properties of the gramicidin A channel. Autocorrelation, spectral power density, relaxation and single-channel studies. *Biochim. Biophys. Acta.* 464:127–141.

Läuger, P. 1978. Transport noise in membranes. Current and voltage fluctuations at equilibrium. *Biochim. Biophys. Acta.* 507:337–349.

Läuger, P. 1983. Conformational transitions of ionic channels. *In* Single-Channel Recording. B. Sakmann and E. Neher, editors. Plenum Publishing Corp., New York. 177–189.

Läuger, P., W. Stephan, and E. Frehland. 1980. Fluctuations of barrier structure in ionic channels. *Biochim. Biophys. Acta* 602:167–180.

Mackay, D. H. J., P. H. Berens, K. R. Wilson, and A. T. Hagler. 1984. Structure and dynamics of ion transport through gramicidin A. *Biophys. J.* 46:229–248.

Neher, E., J. Sandblom, and G. Eisenman. 1978. Ionic selectivity, saturation, and block in gramicidin A channels. II. Saturation behavior of single channel conductances and evidence for the existence of multiple binding sites in the channel. *J. Membr. Biol.* 40:97–116.

Nyquist, H. 1928. Thermal agitation of electric charge in conductors. *Phys. Rev.* 32:110–113.

Ring, A. 1986. Brief closures of gramicidin A channels in lipid bilayer membranes. *Biochim. Biophys. Acta.* 856:646–653.

Ring, A., and J. Sandblom. 1988. Modulation of gramicidin A open channel lifetime by ion occupancy. *Biophys. J.* 53:549–559.

Roux, B., and M. Karplus. 1988. The normal modes of the gramicidin A dimer channel. *Biophys. J.* 53:297–309.

Rudnev, V. S., L. N. Ermishkin, L. A. Fonina, and Y. G. Rovin. 1981. The dependence of the conductance and lifetime of gramicidin channels on the thickness and tension of lipid bilayers. *Biochim. Biophys. Acta.* 642:196–202.

Sandblom, J., G. Eisenman, and J. Hägglund. 1983. Multioccupancy models for single filing ionic channels: theoretical behavior of a four-site channel with three barriers separating the sites. *J. Membr. Biol.* 71:61–78.

Schottky, W. 1918. Über spontane Stromschwankungen in verschiedenen Elektrizitätsleitern. *Ann. Phys. (Leipzig).* 57:541–567.

Sigworth, F. J. 1985. Open channel noise. I. Noise in acetylcholine receptor currents suggests conformational fluctuations. *Biophys. J.* 47:709–720.

Sigworth, F. J. 1986. Open channel noise. II. A test for coupling between current fluctuations and conformational transitions in the acetylcholine receptor. *Biophys. J.* 49:1041–1046.

Sigworth, F. J., and S. Shenkel. 1988. Rapid gating kinetics in gramicidin A channels. *Curr. Top. Membr. Transp.* 33:113–130.

Sigworth, F. J., D. W. Urry, and K. Prasad. 1987. Open channel noise. III. High-resolution recordings show rapid current fluctuations in gramicidin A and four analogues. *Biophys. J.* 52:1055–1064.

Skerra, A., and J. Brickmann. 1987. Simulation of voltage-driven hydrated cation transport through narrow transmembrane channels. *Biophys. J.* 51:977–983.

Urry, D. W. 1971. The gramicidin A transmembrane channel: a proposed $\pi_{LD}$ helix. *Proc. Natl. Acad. Sci. USA.* 68:672–676.

Urry, D. W., T. L. Trapane, and K. U. Prasad. 1983. Is the gramicidin A transmembrane channel single-stranded or double-stranded helix? A simple unequivocal determination. *Science (Wash. DC).* 221:1064–1067.

Urry, D. W., T. L. Trapane, C. M. Venkatachalam, and K. U. Prasad. 1984*a*. C13 nuclear magnetic resonance study of potassium and thallium ion binding to the gramicidin A transmembrane channel. *Can. J. Chem.* 63:1976–1981.

Urry, D. W., S. Alonso-Romanowski, C. M. Venkatachalam, R. J. Bradley, and R. D. Harris. 1984*b*. Temperature dependence of single channel currents and the peptide libration mechanism for ion transport through the gramicidin A transmembrane channel. *J. Membr. Biol.* 81:205–217.

Urry, D. W., S. Alonso-Romanowski, C. M. Venkatachalam, T. L. Trapane, and K. U. Prasad. 1984*c*. The source of the dispersity of gramicidin A single-channel conductances. The L · $Leu^5$-gramicidin A analog. *Biophys. J.* 46:259–266.

Waldbillig, R. C., and G. Szabo. 1979. Planar bilayer membranes from pure lipids. *Biochim. Biophys. Acta.* 557:295–305.

White, S. H. 1978. Formation of "solvent-free" black lipid bilayer membranes from glyceryl monooleate dispersed in squalene. *Biophys. J.* 23:337–347.